THE EFFECT OF MICROSTRUCTURE ON FATIGUE PROPERTIES
OF FERROUS P/M MATERIALS

Tina M. Cimino, Howard G. Rutz, Amie H. Graham, Thomas F. Murphy
Hoeganaes Corporation, Riverton, NJ 08077

ABSTRACT

Fatigue testing (rotating bending fatigue) was performed on several materials in order to evaluate the effect of several microstructural elements. Metallographic analysis was performed to characterize the microstructures of the materials and attempt to identify failure mechanisms.

Previous work indicated that predicting the fatigue strength of P/M materials is a complex relationship between the grain size of the material, the type and strength of the microstructural constituents present and, primarily, the mean pore spacing. [1,2] This study examines these relationships in more depth.

INTRODUCTION

Due to the increasing trends toward higher densities and high performance applications, understanding how the mechanical and fatigue properties of P/M materials are affected by alloying agents and processing techniques is becoming increasingly important. In a previous study [1], fatigue properties at high-density levels appeared to be dictated primarily by pore structures and processing techniques. In particular, mean pore spacing was identified as a major defining element in fatigue performance. Additional studies have been undertaken to better understand the role of porosity and microstructure on fatigue strength.

In the present study, the fatigue properties of FC-0205 [3] conventional premixes with various copper particle size distributions were evaluated. The use of a wide range of copper sizes provided the ability to modify the porosity size and spacing. The results were assessed in relationship to ultimate tensile strength and microstructural constituents other than porosity present in the material. Metallography was performed on the samples to determine the amount and type of constituents present. The pore structures were examined using stereological techniques. The analysis helped build relationships between fatigue life, density, pore structure and composition.

MATERIALS AND PROCESSING

Compositions of the premixes utilized in this study are detailed in Table I. In order to generate the various copper sizes utilized in this study, a sample of ACuMet -200 mesh atomized copper was screened into three distinct particle size ranges. The graphite utilized in the study was Asbury 3203 SCR HS and each mix was made with an addition of 0.75 w/o of Lonza Acrawax. The iron utilized in the study was Ancorsteel® 1000.

Fatigue and tensile samples for materials A, B and C were compacted (ambient temperature) at various pressures. Specimens were sintered in a 75 v/o H2/25 v/o N2 atmosphere for thirty minutes at a temperature of 2050°F (1120°C) or 2300°F (1260°C).

Dogbone specimens for tensile testing were utilized as compacted while the fatigue specimens were machined and ground to size, from a 0.45 inch x 0.45 inch x 3.5 inch nominal sized specimen, following the sintering operation.

Following compaction and sinterin9, density was determined on representative samples by the immersion method outlined in MPIF Standard 42 [4]. The as-sintered tensile properties were determined according to MPIF Standard 10 [4] utilizing a 60,000-pound Tinius Olsen universal tensile tester.

Fatigue specimens utilized in the study were machined to the shape and dimensions outlined Figure 1. Testing was performed on six randomly selected Fatigue Dynamics RBF-200 machines' at a rotational speed of 8000 rpm. A "runout" for the test was considered to be 107 cycles. The staircase method of testing was regulated so that there were both failures and "runouts" at a minimum of two stress levels. The percentage of failures for each stress level was calculated and plotted on a log-normal graph. From these plots, the fatigue endurance limit (FEL) at 50% and 99.9% was determined by linear extrapolation. The 50% FEL represents the stress level where 50% of the specimens will break and 50% will "runout". The 999% FEL represents the stress level where 99.9% of the specimens will "runout" and 0.1% will break.

RESULTS

The tensile and fatigue properties, as well as the 50% FEL as a percent of the ultimate tensile strength for mixes A, B and C at sintering temperatures of 2050°F (1120°F) and 2300°F (1260°C) are summarized in Table II. It should be noted that due to the variability between specimen types, the density of the tensile specimens did not exactly match that of the fatigue specimens. To correlate the data, tensile properties were extrapolated from available data.

Specimens for materials A, B and C underwent metallographic analysis. Optical microscopy was conducted in the unetched and etched conditions. Pore structures of the unetched microstructures were analyzed with a Leitz TAS+ automated image analysis system according to established techniques by Delloff and Aigeltinger[5]. Results of the stereological analysis, which determined mean pore spacing, number of pores per unit area, pore size and pore shape are summarized in Table III. Pore shape was determined by the *form* factor:

$$\text{Form factor} = 4 \pi A / P:$$

W
her

1

e: [5]

A = Area of pore
P = Circumference of pore in plane of analysis

A shape factor of 1 represents a spherical pore, and as the number decreases from 1, the degree of irregularity increases. The form factor is capable of predicting the degree of irregularity, but cannot determine symmetry. Pore shape of Mixes A, B and C is plotted in Figures 2 and 3.

Etched samples were used to determine the constituents present in the samples. Visual point counts were performed on the samples (20 fields per samples) to determine the amount of pearlite and ferrite present. For these analyses, the porosity was considered to be part of the microstructure. It would be necessary to remove the amount of porosity appropriate for the part density to convert the reported numbers to the percentage of metallic phases present. Results are summarized in Table IV.

DISCUSSION

Sintered Density and Sintering Temperature

Sintered density is plotted versus 50% FEL in Figure 4. In all six cases, the fatigue strength was improved with increasing density. However, on average, Mix C showed the smallest improvement of 50% FEL with density. At a sintering temperature of 2050°F (1120°C), Mixes A and B show approximate increases of 2800 and 3300 psi (19.3 and 22.8 MPa), respectively for each 0.1 g/cm^3 increase in density, whereas Mix C shows an approximate increase of only 600 psi (4.1 MPa) for each 0.1 g/cm^3 increase in density. At the higher sintering temperature of 2300°F (1260°C), Mixes A, B and C show approximate improvements in 50% FEL of 4900, 2400 and 1900 psi (33.8, 16.5 and 13.1 MPa) respectively for each 0.1 g/cm^s increase in sintered density. This indicates that in general, the influence of density on 50% FEL is stronger with increasing copper particle size and increasing sintering temperature.

In this study, generally, as the sintering temperature was increased, fatigue performance also increased for a given density level. Previous analysis indicated that, for nickel containing materials, in cases where materials were sintered at two sintering temperatures, materials sintered at the lower sintering temperature had higher fatigue properties for a given density. [1] With the exception of the Low-density properties of Mix A, this study did not correlate with those findings. This may indicate that this trend is a phenomena of nickel containing materials. [2] It is theorized that the behavior of Mix A may be due to the more dominant combination of Low density and the number of large pores present in this material. The effect of porosity is discussed in more detail below.

Ultimate Tensile Strength

The relationship between ultimate tensile strength and 50% FEL for Mixes A, B and C is shown in Figure 5. The data, summarized in Table III, was considered of particular interest because although the composition of the test materials was constant, as the copper particle size decreased, the 50% FEL was not a consistent percentage of the ultimate tensile strength. For sintering temperatures of 2050°F (1120°C) and 2300°F (1260°C), the plot indicates that at lower density levels, the 50% FEL tends to increase with decreasing copper particle size. For example, at 2050°F (1120°F) and 30 tsi (415 MPa), Mix C shows a 50% FEL approximately 17% higher than that of Mix A. This percentage is approximately 20% at a sintering temperature of 2300°F (1260°C). Also, as the copper particle size decreased, the 50% FEL represented an increasing percentage of the ultimate tensile strength. At a sintering temperature of 2050°F (1120°C) and a compaction pressure of 45 tsi (620 MPa), the corresponding increase in 50% FEL with decreasing copper particle size is 5% and 6% respectively for sintering temperatures of 2050°F (1120°C) and 2300°F (1260°C), and the 50% FEL represents a fairly consistent percentage of the ultimate tensile strength. This would indicate that the admixed copper particle size has a stronger effect on the fatigue endurance limit at lower density levels.

Optical Microscopy

The unetched pore structures of materials A, B and C at compaction pressures of 30 tsi (415 MPa) and 50 tsi (690 MPa) are shown in Figure 6. In theory, copper reaches liquid phase during conventional sintering at 2050°F (1120°C), (copper melting point = 1983°F {1084°C}) and diffuses rapidly into the iron matrix, leaving behind pores where the copper particles resided. The photomicrographs indicate that, as expected, the pore structure after sintering is directly related to the copper particle size, with the number of large pores decreasing with decreasing copper particle size. Stereological analysis was done to quantify the difference in the pore structures.

Stereological Parameters

Several stereological parameters including, pore shape, mean pore spacing, number of pores per unit area, and pore size were examined to determine if the pore structure had any effect on the fatigue properties.

Plots of pore shape at sintering temperatures of 2050°F/1120°C and 2300°F/1260°C (Figures 2 and 3) indicated that, as expected, with increasing sintering temperature the pore shape tends toward spherical. The pore shapes of Mixes A, B and C become comparable and more uniform as the sintering temperature is increased to 2300°F (1260°C). Overall, variations in the copper particle size appeared to have no effect upon the pore shape of the samples.

The copper particle size appeared to have no significant effect upon the number of pores per unit area. However, an effect can be seen when the cumulative % pore size, plotted at a compaction pressure of 45 tsi (620 MPa) in Figure 7, is examined. In general, the number of significantly large pores (> 2400 μm) increases with increasing particle size and sintering temperature. For example, at a sintering temperature of 2050°F (1120°C), the number of pores greater than

2400 μm for Mixes A, B and C is 6.4%, 3.5% and 2.3%, respectively. Increasing the sintering temperature to 2300°F (1260°C) results in percentages of 12.5% for Mix A, 6.3% for Mix B and 1.2% Mix C.

Mean pore spacing, when compared with sintered density, tended to show a slight decrease with decreasing particle size, with the exception of samples that were compacted at a pressure of 30 tsi (415 MPa) and sintering temperature of 2050°F (1120°F), where the

mean pore spacing was constant. However, there appears to be a relationship between mean pore spacing and 50% FEL, which is plotted in Figure 8. The data shows that, for a given material, as the 50% FEL increases the mean pore spacing increases. This correlates with the previous analysis that was conducted on a range of alloy systems, but the relationship does not appear to be as strong. [1]

For the present analysis, the stereological parameters that appeared to have a relationship with endurance limit were mean pore spacing and pore size.

Microstructure

At a sintering temperature of 2050°F (1120°C) and compaction pressure of 30 tsi (415 MPa), the amount of ferrite present decreased with decreasing copper particle size. The trend, although not as pronounced, is present at the higher sintering temperature of 2300°F (1260°C). This is evident when examining the photomicrographs of Mixes A and C at 30 tsi (415MPa) which are shown in Figure 9. The photomicrographs clearly show microstructural differences between the materials. The difference in ferrite content may be related to the sintered carbon content of the material. The data, detailed in Table VII, indicates the sintered carbon content of Mixes A and B is comparable, while the carbon content of Mix C is 0.05 w/o to 0.09 w/o higher.

Photomicrographs of the fatigue crack propagation for Mixes A and C at a compaction pressure of 30 tsi (415 MPa) and a sintering temperature of 2300°F (1260°C) are shown in Figure 10. The evidence of very large pores in Mix A and the difference in ferrite content is apparent. There does appear to be a slightly higher concentration of pores along the crack length for Mix A.

The other possible influence on the fatigue endurance limit is copper diffusion. Differential Thermal Analysis that was conducted on the copper samples indicated no significant difference in the melting point of the copper used for Mixes A, B and C within the measuring error of the equipment. However, it is possible that the large copper rich areas in Mix A acted to hinder the carbon diffusion, resulting in a higher percentage of ferrite.

In summary, this study indicates that determining the fatigue endurance limit of a material is much more complex than simply assuming it is a fixed percentage of the ultimate tensile strength. There is a strong indication that pore size and mean pore spacing are important stereological parameters for predicting the fatigue endurance limit of the FC-0205 materials that were examined. There also appears to be a relationship between the fatigue endurance limit and the microstructural constituents present. The stereological parameters appeared to have a much stronger influence than the microstructural constituents do on the fatigue properties as the copper particle size increased and density levels decreased. The extent of the microstructural influence cannot be confirmed without more detailed analysis, but it appears to have a stronger influence at the higher density levels. All the samples for this study were sintered in a laboratory scale pusher furnace. Future work should include examining the mechanical and fatigue properties of the FC-0205 materials when sintered in a production belt furnace with a preheat zone to ensure more complete copper diffusion.

CONCLUSIONS

1. As the density of the FC-0205 premixes was increased, the fatigue properties increased. The increase in 50% FEL with density was more pronounced with increasing sintering temperature and increasing copper particle size.

2. The 50% FEL as a function of ultimate tensile strength was primarily affected by copper particle size at Low compaction pressures, and became independent of copper particle size at higher compaction pressures. This correlated with previous analysis which indicated that fatigue endurance limit is not simply a fixed percentage of the ultimate tensile strength.

3. Difference in copper particle size had no significant effect upon pore shape or number of pores per unit area but did have a significant influence on pore size.

4. The 50% FEL of the FC-0205 materials examined appeared to be related to both pore size and mean pore spacing. The influence of pore size and mean pore spacing on the fatigue endurance limit was strongest at the lowest density levels, This may indicate that the fatigue endurance limit is related to the largest pore present in the sample.

5. There appears to be a relationship between microstructural constituents and the fatigue endurance limit. However, due to the variation in carbon content and copper diffusion of the test materials, the degree to which it influenced the properties is inconclusive.

ACKNOWLEDGMENTS

REFERENCES

1. Rutz, H.G., Murphy, T.M., Cimino. T.M., "The Effect of Microstructure on Fatigue Properties of High Density Ferrous Materials", *Advances in Powder Metallurgy and Parb'culate Materials-lgg6,* Vol. 4, pp 13-375 13-389, Metal Powder Industries Federation,
2. Princeton, NJ.

3. O'Brien, R.C, "Fatigue Properties of P/M Materials", SAE Technical Paper 880165, 1988, Society of Automotive Engineers, Cobo Hall, Detroit, Michigan.

4. "MPIF Standard 35 - Materials Standards for P/M Structural Parts", Metal Industries Federation, Princeton, NJ, 1994.

5. "Standard Test Methods for Metal Powders and Powder Metallurgy Products", Metal Industries Federation, Princeton, NJ, 1996.

6. Delloff, R.T., Aigeltinger, E.H., "Experimental Quantitative Microscopy with Special Applications to Sintering", Perspectives in Powder Metallurgy--Volume 5--Advanced Experimental Techniques in Powder Metallurgy, pp 81-137, Plenum Press, New York--London, 1970.
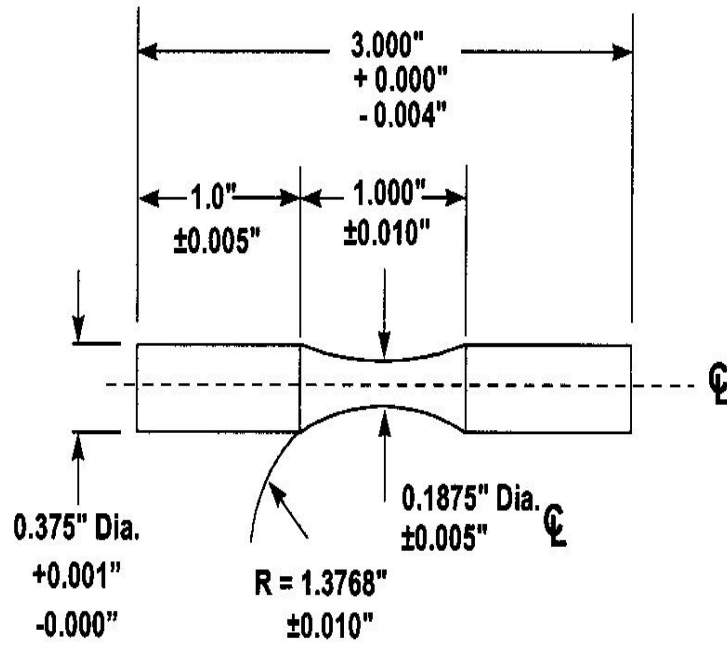
Figure 1:   Specification of Rotating Bending Fatigue Specimen

Table II: Fatigue and Tensile Properties for FC-0205 Premixes Sintered at 2050°F (1120°C) / 2300°F (1260°C)

Material	Sintering Temperature (°F / °C)	Density (g/cm³)	UTS (10³ psi / MPa)	50% FEL (10³ psi / MPa)	99.9% FEL (10³ psi / MPa)	50% FEL as % UTS
A	2050 / 1120	6.89	70.0/483	25.3/174	20.3/140	36.2
		7.06	79.3/547	30.0/207	23.6/163	37.9
B		6.87	69.2/477	25.0/172	20.8/143	36.1
		7.07	78.6/542	31.6/218	25.8/178	40.1
C		6.89	72.3/498	30.6/211	24.5/169	42.3
		7.08	80.0/552	31.7/219	26.9/185	39.6
A	2300 / 1260	6.97	72.4/499	25.7/177	20.4/141	35.5
		7.14	80.0/552	34.1/235	28.4/196	42.6
B		6.94	73.0/503	29.6/204	23.4/161	40.5
		7.15	81.5/562	34.7/239	27.8/192	42.5
C		6.95	73.7/508	32.1/221	27.8/192	43.5
		7.16	87.0/600	36.1/249	29.4/203	41.4

Table III: Stereological Data of FC-0205 Premixes Sintered at 2050°F (1120°C) / 2300°F (1260°C)

Material	Sintering Temperature (°F / °C)	Density (g/cm³)	Mean Pore Spacing (µm)	Number of Pores per 1000 µm²
A	2050 / 1120	6.89	54	107
		7.06	63	118
B		6.87	55	110
		7.07	59	124
C		6.89	55	99
		7.08	59	119
A	2300 / 1260	6.97	65	95
		7.14	71	116
B		6.94	63	93
		7.15	70	107
C		6.95	60	97
		7.16	65	113

Table IV: Microstructural Analysis of FC-0205 Premixes - Sintering Temperatures 2050°F (1120°C) / 2300°F (1260°C)

Material	Sintering Temperature (°F / °C)	Density (g/cm³)	% Constituents	
			Pearlite	Ferrite
A	2050 / 1120	6.89	58.3	28.6
B		6.87	64.3	22.2
C		6.89	67.5	20.5
A	2300 / 1260	6.97	57.0	32.4
B		6.94	63.7	26.2
C		6.95	61.5	28.8

4
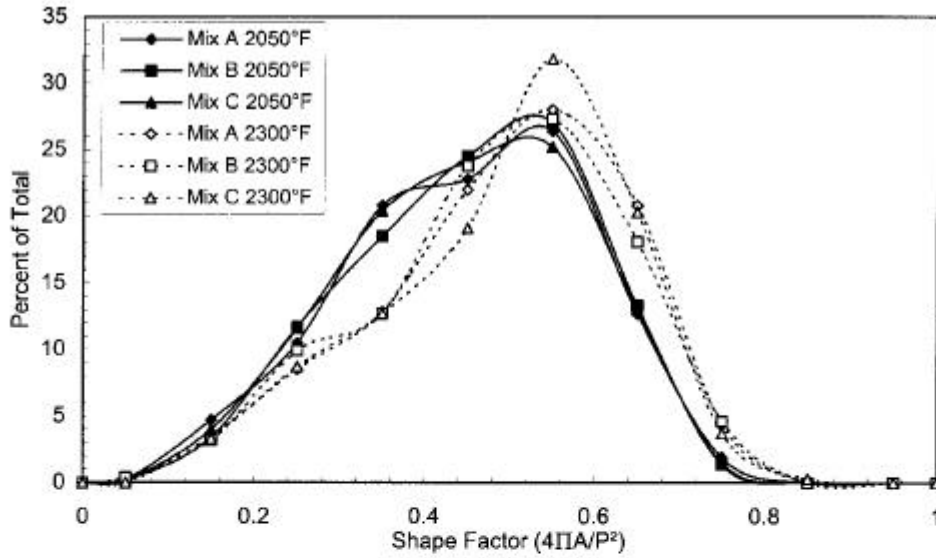
Figure 2: Pore Shape of FC-0205 Premixes - Compaction Pressure 30 tsi / 415 MPa
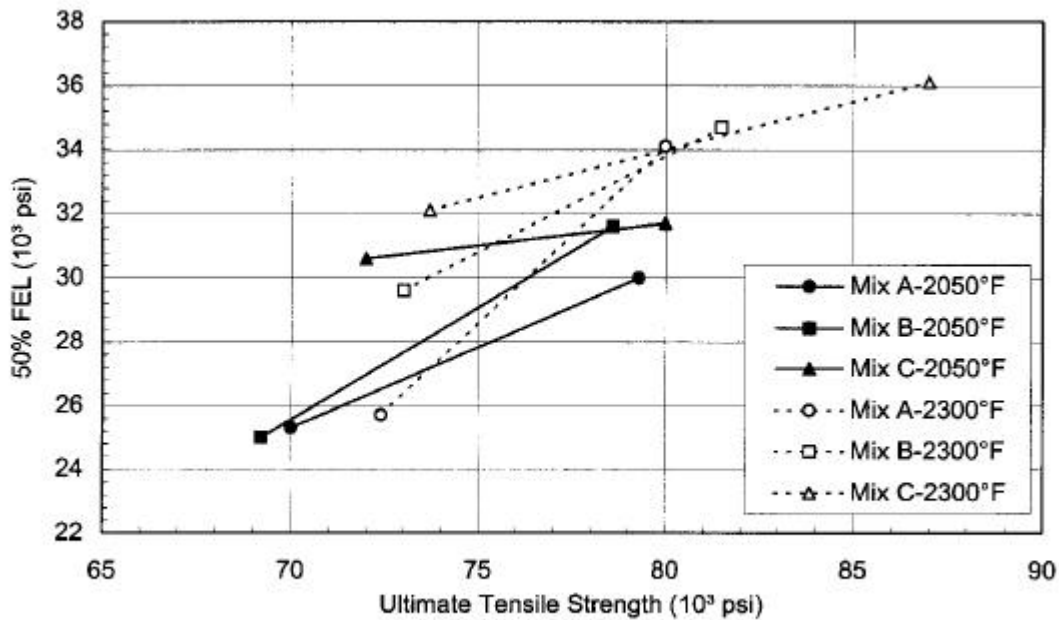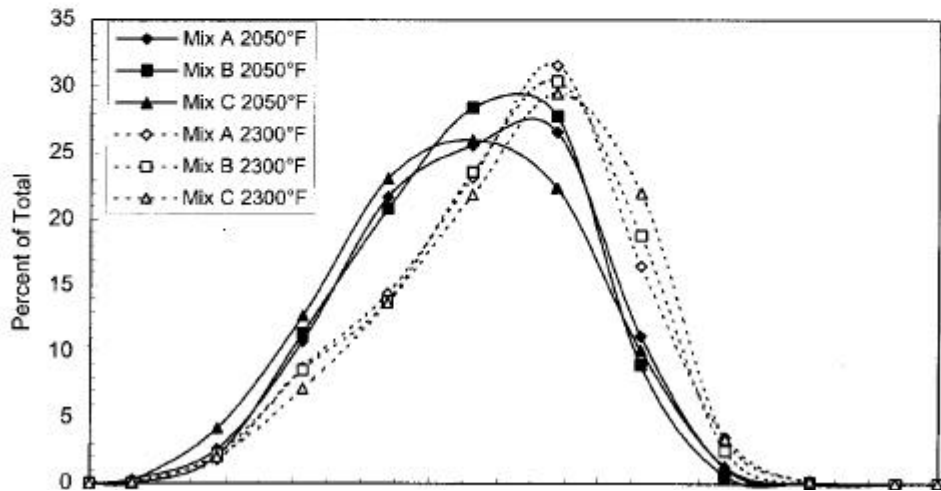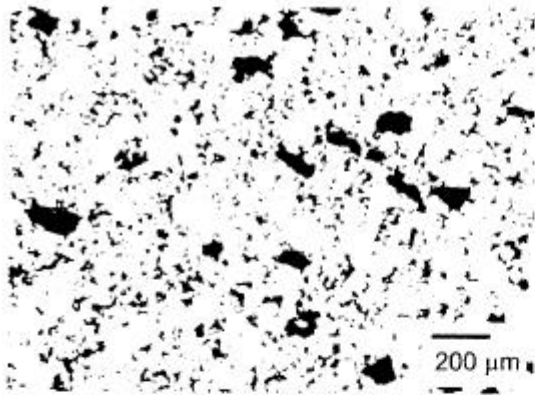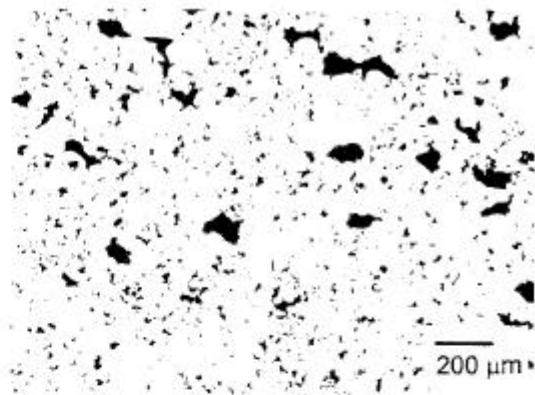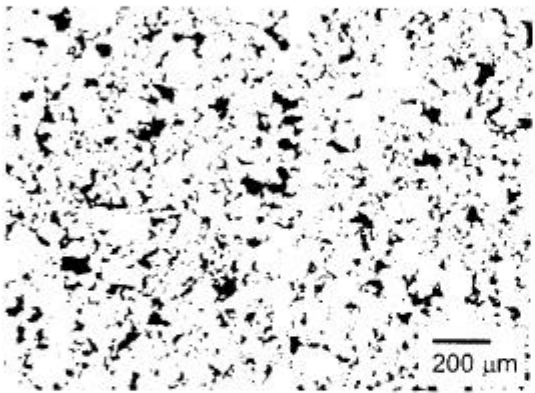

Figure 5: Ultimate Tensile Strength versus Fatigue Endurance Limit for the
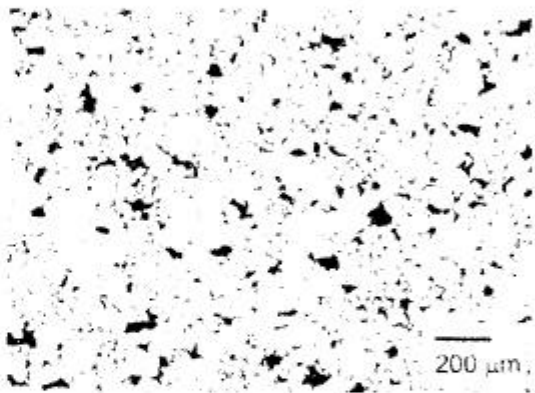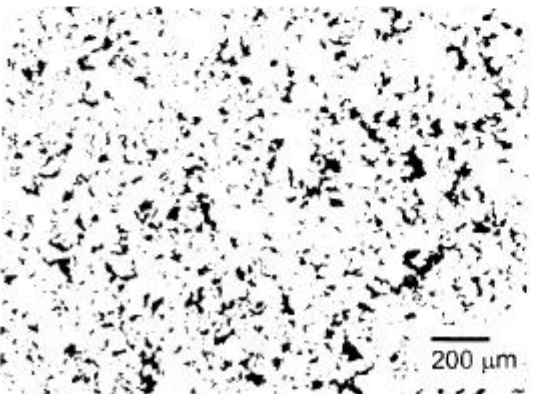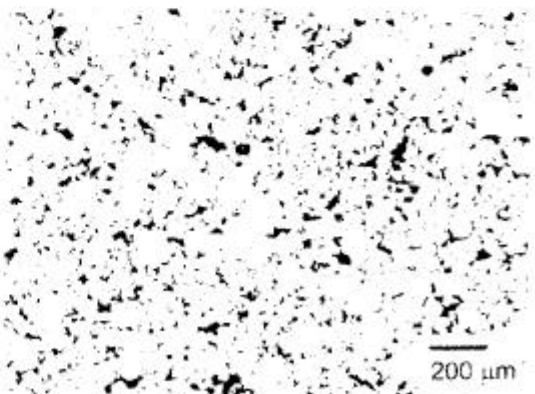
Mix A – 30 tsi (415 MPa)

Mix A – 50 tsi (690 MPa)

Mix B – 30 tsi (415 MPa)

Mix B – 50 tsi (690 MPa)

Mix C – 30 tsi (415 MPa)

Mix C – 50 tsi (690 MPa)

Figure 6: Photomicrographs of Unetched Pore Structure of FC-0205 Premixes
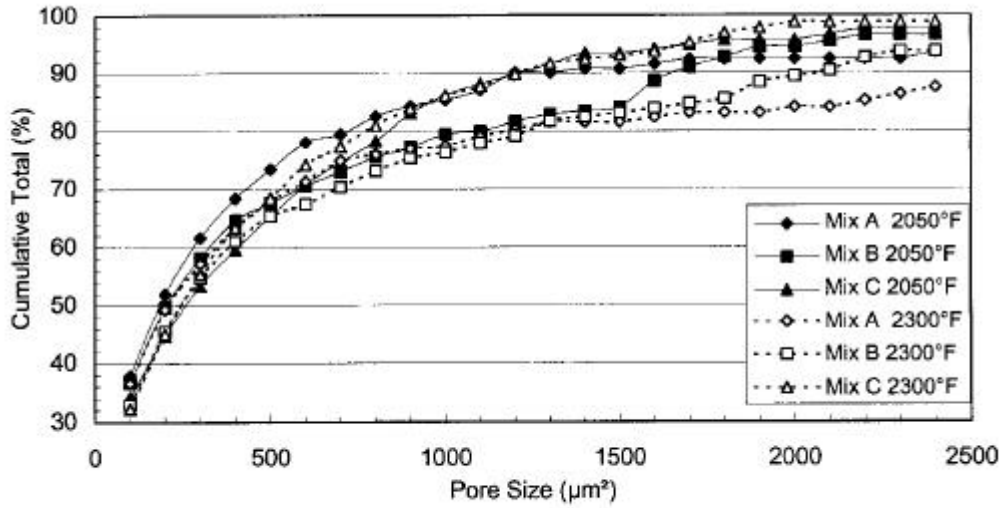Sintering Temperature - 2050°F (1120°C), Original Magnification 50x

8

Figure 7: Pore Size versus Cumulative Total % - Sintering Temperatures 2050°F (1120°C) /2300°F (1260°C)
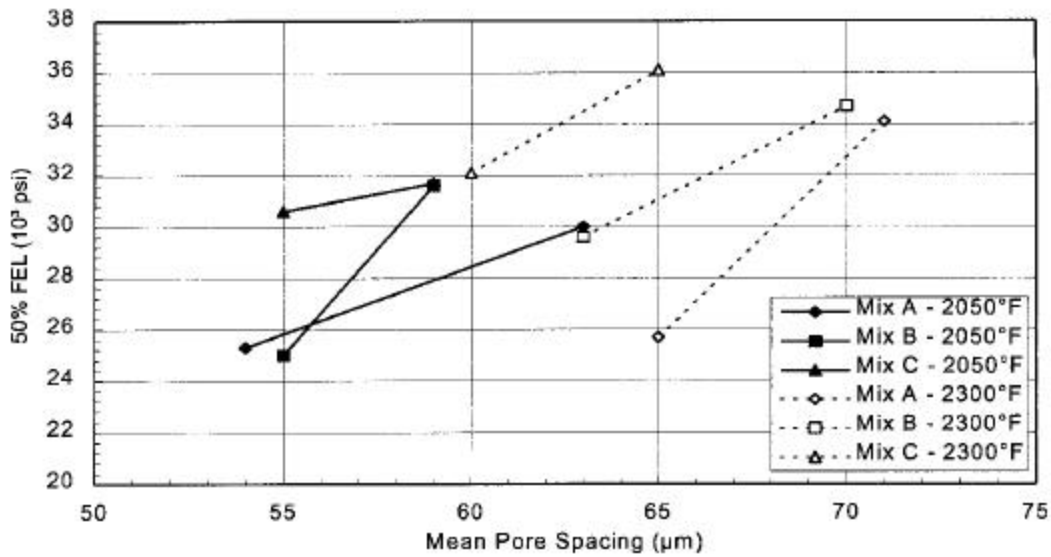
Figure 8: Mean Pore Spacing vs. 50% FEL for FC-0205 Premixes

Table V: Sintered Carbon of FC-0205 Premixes

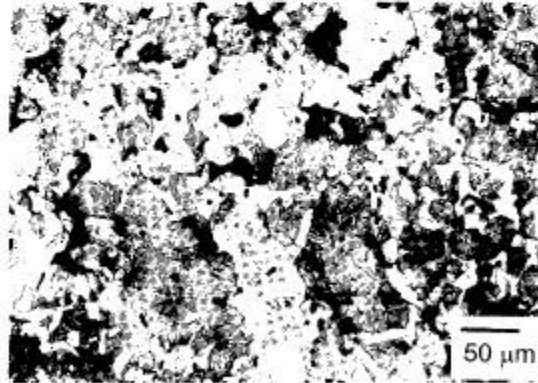| Material	Sintering Temperature (°F / °C)	Sintered Carbon (w/o)
A	2050 / 1120	0.66
B		0.64
C		0.73
A	2300 / 1260	0.65
B		0.69
C		0.70
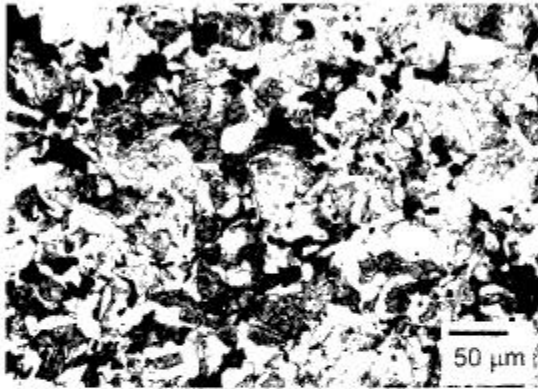
Mix A – 30 tsi (415 MPa)
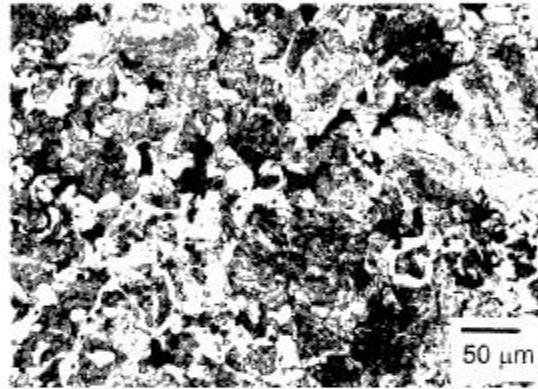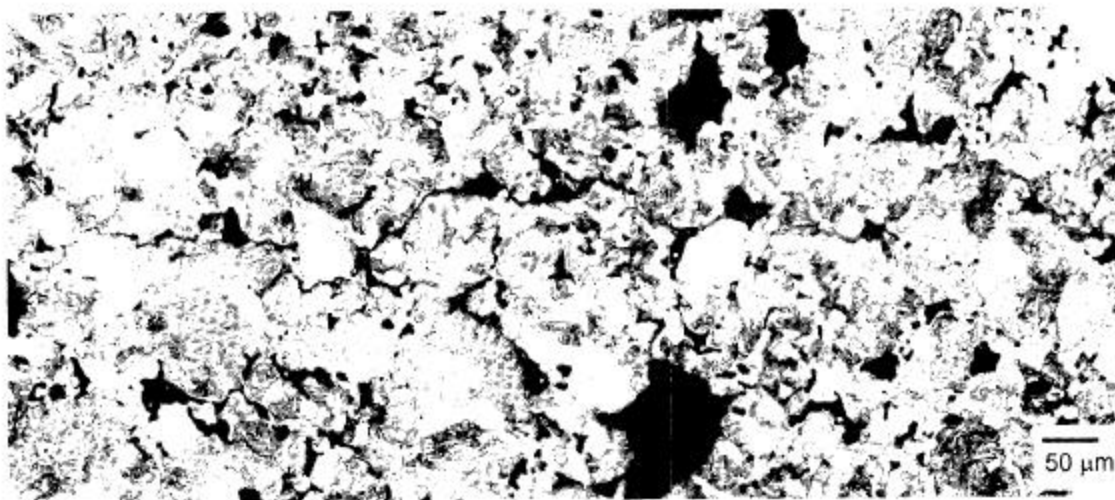
Mix A – 45 tsi (620 MPa)
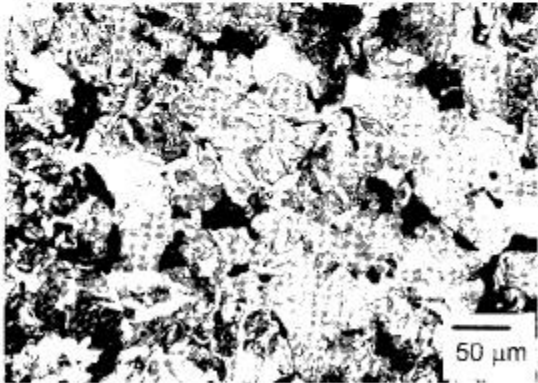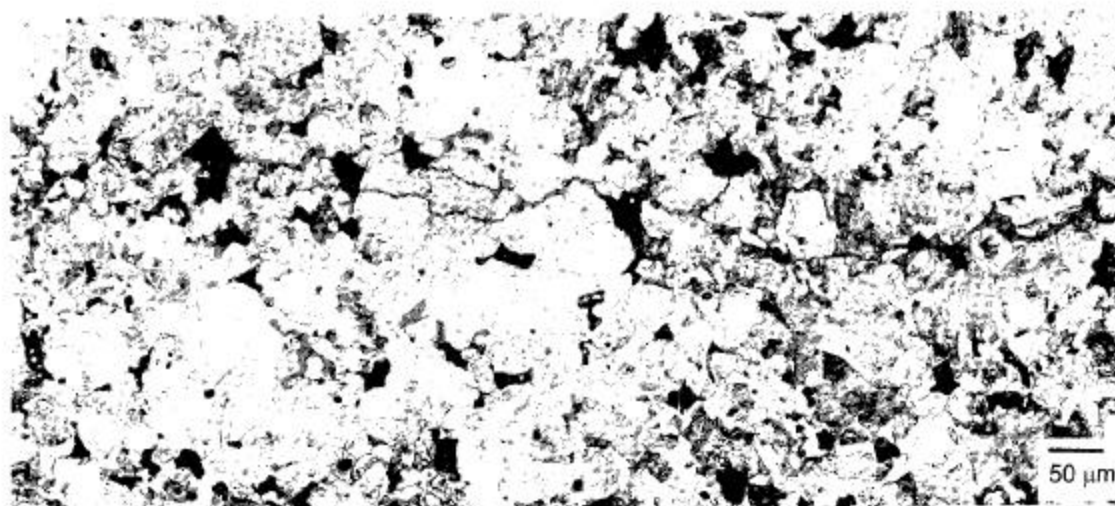
Mix C – 30 tsi (415 MPa)

Mix C – 45 tsi (620 MPa)

Figure 9: Photomicrographs of Etched Microstructure - FC-0205 Premixes
Sintering Temperature -- 2300°F (1260°C), Original Magnification 200x

Mix A – 30 tsi (415 MPa)

Mix C – 30 tsi (415 MPa)

Figure 10:   Photomicrographs of crack propagation - FC-0205 Premixes Sintering
Temperature 2050°F (1120°C) / 2300°F (1260°C), Original Magnification 200x